JOURNAL OF Applied Polymer SCIENCE

# Hydrophobically Associating Acrylamide-Based Copolymer for Chemically Enhanced Oil Recovery

**Zhongbin Ye,[1,2] Mingming Feng,[2] Shaohua Gou,[1,2] Man Liu,[2] Ziyan Huang,[2] Tongyi Liu[1,2]**

[1]State Key Laboratory of Oil and Gas Reservoir Geology and Exploitation, Southwest Petroleum University, Chengdu 610500, People's Republic of China

[2]School of Chemistry and Chemical Engineering, Southwest Petroleum University, Chengdu 610500, People's Republic of China

Correspondence to: S. Gou (E-mail: shaohuagou@swpu.edu.cn)

**ABSTRACT:** A hydrophobically associating copolymer was prepared by free-radical polymerization with acrylamide (AM), acrylic acid (AA), and *N*-allyloctadec-9-enamide (NAE) as monomers. The structure was characterized by Fourier transform infrared spectroscopy, $^{1}$H-NMR, $^{13}$C-NMR, and scanning electron microscopy. The rheological experiments indicated that the copolymer possessed superior properties compared with partially hydrolyzed polyacryamide. It was found that an AM/AA/NAE/Tween-80 system could effectively decrease the interfacial tension and reduce the surfactant loss caused by stratum adsorption in polymer–surfactant flooding.
 J. Appl. Polym. Sci. 000: 000–000, 2013

**KEYWORDS:** adsorption; properties and characterization; rheology

Received 27 December 2012; accepted 15 April 2013; Published online
**DOI: 10.1002/app.39424**

## INTRODUCTION

Hydrophobically associating water-soluble polymers (HAWSPs) have attracted much attention because of their unique structures and properties, including their thickening properties, shear thinning, and antipolyelectrolyte behavior which have been widely investigated in oil chemistry additives such as mobility control agents and rheology modifiers.[1–9] Designing and developing a series of efficient polymer structure is significant for oil and gas exploitation. Therefore, a remarkable number of HAWSPs, including *N*-(4-ethyl) phenyl acrylamide and acrylamide (AM) copolymer,[10] methyl acrylic acid-2-dimethylamino ethyl acrylate and methyl *tert*-butyl ester copolymer,[11] methyl acrylic acid, ethyl acrylate and poly(ethylene oxide) (PEO) copolymer (Hydrophobically modified alkali-soluble emulsion polymers, HASE Ps),[12] and $PEO_{99}$–poly(propylene oxide)$_{67}$–$PEO_{99}$ (F127) multiblock copolymers,[13] have been developed since the 1980s.[14]

As we know, the reduction of the interfacial tension among oil, water, and rocks should be paid more attention when the polymer flooding strategy is used in an oil reservoir. However, HAWSPs cannot effectively reduce the interfacial tension among oil, water, and rocks.[15] A large number of authors have indicated that a polymer solution adjusting a certain amount of surfactant (polymer–surfactant system) could reduce the interfacial tension significantly.[16–19] The flooding procedure model of a HAWSP–surfactant system is shown in Figure 1. Surfactants and HAWSPs interact by electrostatic interactions and hydrophobic interactions. Electrostatic interactions would be caused by hydrophobic associations between polymer hydrophobic moieties and the hydrophobic tail of the surfactant. Hydrophobic interactions could be explained by cooperative interactions and Coulomb attractions of the polymer chains and the ionic/nonionic surfactant.[20–23]

Because the interaction between the surfactant and HAWSPs could reduce the interfacial tension, a novel enhanced oil recovery chemical, AM/acrylic acid (AA)/*N*-allyloctadec-9-enamide (NAE), was designed via the introduction of NAE structural units into the AM-based copolymer. The combination systems of copolymer solution and surfactants were investigated which included shear resistance, temperature tolerance, salt compatibility, and low interfacial tension.

## EXPERIMENTAL

### Materials

AM, AA, poly(oxyethylene octylphenol ether) (OP-10), sodium hydrogen sulfite ($NaHSO_3$), ammonium persulfate [$(NH_4)_2S_2O_8$], anhydrous sodium sulfate, oleic acid, allyl bromide, phosphorus trichloride, triethylamine, sodium chloride (NaCl), magnesium chloride hexahydrate ($MgCl_2{\cdot}6H_2O$), anhydrous calcium chloride ($CaCl_2$), cetyltrimethyl ammonium

Additional Supporting Information may be found in the online version of this article.

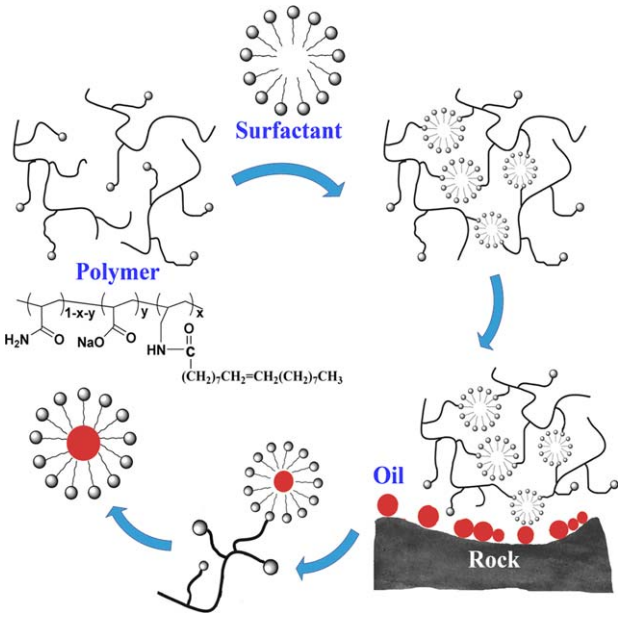


**Figure 1.** Model of the flooding procedure of the HAWSP–surfactant system. [Color figure can be viewed in the online issue, which is available at www.interscience.wiley.com.]

bromide (CTAB; cationic surfactant), sodium dodecyl sulfate (SDS; anionic surfactant), polyoxyethylene(80) sorbitan monooleate (Tween-80, nonionic surfactant), and ethanol were analytical reagent grade and were used directly without further purification. All of the reagents were purchased from Chendu Kelong Chemical Reagent Factory (China). The viscosity-average molecular weight of partially hydrolyzed polyacryamide (HPAM) was about $5.0 \times 10^6$; it was purchased from Chengdu Kelong Chemical Reagent Factory. Deionized water and fresh water were obtained by an ion-exchange method. NAE was synthesized according to the literature.[24,25]

### Preparation of AM/AA/NAE

AM/AA/NAE was synthesized by the following procedure. An indicated amount of NAE, deionized water, and OP-10 were placed in a 250-mL, three-necked flask with stirring for 10 min at 25°C. Then, AM and AA were added (the concentration of the polymerizing system was 20 wt %), and the pH of system was adjusted to the indicated value by an NaOH (2.0*M*) solution. The system solution was fended nitrogen gas for 20 min at 25°C. The initiator, $(NH_4)_2S_2O_8$, and $NaHSO_3$ were added after 30 min. The polymerization was maintained at 40°C for 8 h after nitrogen gas had been bubbled through the solution about 20 minutes. AM/AA/NAE was obtained after we washed the transparent gel five times with 50 mL of ethanol until a white block solid precipitated. The solid was further crushed and dried in an oven at 40°C for 2 days.

### Characterization

The Fourier transform infrared (FTIR) spectrum was obtained with a PerkinElmer IR 883 instrument (Beaconsfield, United Kingdom) in the optical range 400–4000 $cm^{-1}$ by the averaging of 32 scans at a resolution of 4 $cm^{-1}$ with the samples in KBr pellets. $^1$H-NMR and $^{13}$C-NMR spectra were detected by a 400-MHz Bruker NMR spectrometer after the sample was dissolved in $D_2O$.

### Scanning Electron Microscopy (SEM)

To observe the surface morphology of the samples, a Quanta450 SEM instrument (Fez Co.) was used. The resolution was 3 $\mu$m, and the magnifying multiples ranged from 3 to 30,000. Analysis was achieved at an acceleration voltage of 20 kV and a pressure of 120–500 Pa in the sample chamber. First, AM/AA/NAE and HPAM were dissolved in the deionized water at a concentration of 2000 mg/L, and then, the solutions were kept for 48 h at 25°C to reach equilibrium. The samples were then frozen in liquid nitrogen. The cross sections were imaged at an accelerating voltage of 20 keV, and the specimen was scanned at magnifying multiples of 2000 and 5000 to obtain clear morphological information.

### Rheological Experiments

The temperature tolerance and shear resistance of the copolymers in aqueous solutions were investigated by a stress-controlled rheometer (Haake RheoStress6000, Germany) equipped with cone/plate geometry (diameter = 60 mm, angle = 1°, plate-to-plate gap = 0.104 mm). The temperature was adjusted by standard silicon oil within the range 25–120°C.

### Solution Viscosity, Conversion Rate, and Intrinsic Viscosity

The solution viscosity was measured at 7.34 $s^{-1}$ at 25°C with the help of a Brookfield LVTDV-III viscometer. The conversion of AM/AA/NAE was determined by a high-performance liquid chromatography (HPLC; Prominenece UFL, Shimadzu Corp., Japan) technique in the copolymerization with an external standard method: Octadecylsilyl (ODS) column, UV detector at 210 nm, 1.0 mL/min, and $H_2O/CH_3OH = 90/10$ v/v.[26] Intrinsic viscosity ($[\eta]$) was measured with a 0.6-mm NCY automatic Ubbelohde capillary viscometer (Shanghai Sikeda Scientific Instruments, Inc., Shanghai, China) at 30.0 ± 0.1°C. All of the samples were dissolved with 1 mol/L NaCl and allowed to stand for 4 h to fully distribute.[27]

### Pyrene Fluorescence Probe

To determine the critical association concentration (CAC) of AM/AA/NAE, the relation of viscosity with the concentration was first investigated. After we determined a rough concentration range, a more precise investigation was done with a pyrene fluorescence probe. The fluorescence intensities were measured with a Shimadzu RF-5301PC spectrofluorophotometer. The excitation wavelength was 335 nm, and the emission spectra were scanned over the spectral range 350–550 nm. The slit widths of both excitation and emission were fixed at 5 nm. The thickness of the sample cell was 1 cm. The preparation process of the pyrene probe solutions was performed as follows. First, pyrene (10.112 mg) was dissolved with the methanol as the solvent in a 50-mL volumetric flask, here, the concentration of pyrene was $1 \times 10^{-3}$ mol/L. Then, by a microsyringe, we transferred 250 $\mu$L of the prepared pyrene solution into a 50-mL volumetric flask, passing over nitrogen along the bottle bottom to remove the methanol. After we added an adequate amount of polymer in the volumetric flask, it was diluted with distilled water to volume and oscillated by ultrasound for 10 min to disperse the pyrene evenly in the solution. The different

**Table I.** Optimum Conditions for Polymerization

| AM (wt %) | AA (wt %) | NAE (wt %) | OP-10 (wt %) | Temperature (°C) | pH | Reaction time (h) | [η] (mL/g) |
|---|---|---|---|---|---|---|---|
| 16 | 4 | 0.3 | 0.03 | 40 | 7.5 | 8 | 809.6 |

concentrations of polymer solution with pyrene were prepared with the aforementioned method. Finally, all of the solutions were kept for 48 h at 25°C to allow them to reach equilibrium. The final concentration of pyrene was $2 \times 10^{-6}$ mol/L. All of the measurements were performed at 25°C. The ratios between the strength of the first peak ($I_1$) and that of the third peak ($I_3$) in the pyrene emission spectra were calculated.

### Interfacial Tension

Numerous works have indicated that the addition of surfactant to the polymer solution is favorable for reducing the interfacial tension.[28–30] To obtain a superior polymer–surfactant system, the interactions of the copolymer with the different sorts of common surfactants (the cationic surfactant, CTAB; the anionic surfactant, SDS; and the nonionic surfactant, Tween-80) were investigated. The surfactant or the mixture of surfactant and polymer were prepared with deionized water, and the interfacial tensions between solutions and air were measured by a DT-102A fully automated tensiometer with a precision of ±0.1 mN/m at 25°C.

### Adsorption Experiments

In the practical application of oil exploitation, the addition of surfactant to the polymer solution is to reduce interface tension. However, the consumption of surfactant is of great quantity because of the adsorption effect of the porous medium.[31] To explore the potential applications in enhancing oil recovery, the capacity of AM/AA/NAE, which protected the surfactant against the adsorption of strata was examined by measuring the adsorption of mixture composed by surfactant and copolymers. The test was as follows. First, drill cores (10 g) milled into a 40–60 screen mesh were added to a 2-L Erlenmeyer flask. The mixture of solutions and cores was put into a constant-temperature shaker at a speed of 150 rpm for 24 h. Second, the drill cores were removed by a high-speed centrifuge. The peak area of the surfactant in the upper clear liquid [the final solution ($S_X$)] was determined by an HPLC technique with an Octadecylsilyl (ODS) column (UV detector at 220 nm, 1.0 mL/min, and $CH_3OH/H_2O = 95/5$ v/v). The final solution concentration ($C_X$; g/L) was determined by the following equation:

$$C_X = \frac{S_X}{S_{St}} \times C_{St} \quad (1)$$

where $S_{St}$ is the peak area of the known surfactant solution and $C_{St}$ is the concentration of the known surfactant solution. The adsorption quantity of each solution was calculated with the adsorption equation:[32]

$$\Gamma = \frac{(C_0 - C_X)V}{m} \quad (2)$$

where Γ is the adsorbance, $C_0$ is the initial concentration (g/L), $V$ is the volume of the solution (L), and $m$ is the mass of the adsorbent (g).

### Core Flood Test

The core assembly was a stainless steel cylinder with a length of 25 cm and an internal diameter of 2.5 cm packed with sand. We obtained the sand by grinding iron-free sandstone and further purified iron impurities by washing it with hot hydrochloric acid and then washing it with distilled water for 2 h at 30°C. The differential pressures between the inlet and the outlet during the recovery were monitored. After the packed dry core apparatus was assembled, the sand pack was saturated with distilled water. The simulation crude oil was collected from Shengli oil field (China), after dehydration with a density of 0.90 g/cm$^3$, apparent viscosity of 70.34 mPa s at 65°C. An ISCO260D syringe pump was used at a maximum injection pressure of 50 MPa with an accuracy of 0.1% FS.

## RESULTS AND DISCUSSION

### Optimum Conditions for the Copolymerization of AM/AA/NAE

To obtain the optimum polymerization conditions, the effects of the ratio of AM to AA, NAE, emulsifier loading, reaction temperature, pH, and reaction time were investigated by the single-variable method.[15] First, we kept the loadings of NAE at 0.1 wt %, OP-10 at 0.03 wt %, and the initiator at 0.05 wt %, and then ensuring the pH, reaction time, and monomer content as fixed values, we changed the temperature of the system to investigate the influence of the reaction temperature on polymerization by observing the apparent viscosity. On the basis of the aforementioned approach, the effects of other factors on polymerization were studied. The results are summarized in Table I.

### FTIR Spectra Analysis

The FTIR spectra of HPAM, AM/AA/NAE, and the NAE monomer are shown in Figure 2. In the spectrum of NAE, strong absorption peaks were observed at 3292 and 1659 cm$^{-1}$; these were attributed to the stretching vibrations of N—H and C═O bonds, respectively, in the —$CONH_2$ group. The peak at 1548 cm$^{-1}$ was due to the stretching vibrations of C═C, and those at 2922 and 2856 cm$^{-1}$ were assigned to the stretching vibrations of C—H bond in the —$CH_2CH_3$ group. The IR spectrum of AM/AA/NAE presented two peaks in 2946 and 2856 cm$^{-1}$; this indicated that the NAE structure was successfully introduced into the macromolecule chain. In addition, the stretching vibrations of O—H, N—H, and C═O were confirmed by characteristic absorptions at 3478, 3196, and 1677 cm$^{-1}$; this demonstrated that the structures of AM and AA existed in the copolymer. Thus, we concluded that the polymer contained the structures of AM, AA, and NAE.[26]

### $^1$H-NMR and $^{13}$C-NMR Analysis

The $^1$H-NMR spectra of AM/AA/NAE are presented in Figure 3(a). The chemical shift value at about 7.6 ppm was assigned to the NH protons of —$CONHCH_2$—. The chemical shift value at

Applied Polymer SCIENCE

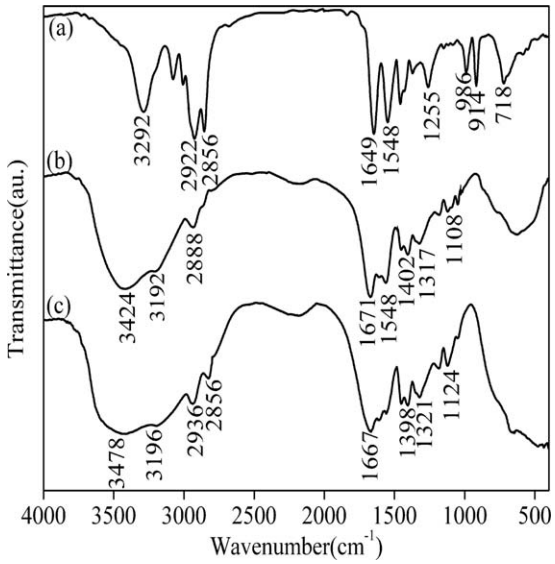


**Figure 2.** FTIR spectra of (a) NAE, (b) HPAM, and (c) AM/AA/NAE.

6.0 ppm was due to the NH protons of $NH_2COCH_2$— in the amide unit. The chemical shift value at 5.5–5.6 ppm was due to the CH protons of —CH=CH— in the aliphatic chain. The protons of the $—CH_2—$ of $—CH_2NH—$ exhibited a signal at 3.5–3.6 ppm. The protons of the aliphatic —CH— of the polymeric chain appeared at 1.8–2.5 ppm. The protons of the aliphatic $—CH_2—$ of the polymeric chain and aliphatic chain appeared at 1.2–2.4 ppm. The chemical shift of the CH proton of $—CH_3$ in the aliphatic chain was at 1.06–1.09 ppm.[26]

The $^{13}$C-NMR spectrum of AM/AA/NAE is shown in Figure 3(b). The chemical shift value at about 16.9 ppm was assigned to the C proton of $—CH_3$ in the aliphatic chain. The chemical shift value at 25.0–47.0 ppm was due to the C protons of the aliphatic $—CH_2—$ and —CH— of the polymeric chain and aliphatic chain. The chemical shift value at 126.5–133.5 ppm was due to the C protons of —CH=CH— in the aliphatic chain. The C protons of —CONH—, —COONa, and $—CONH_2$ exhibited a signal at 179.4–183.8 ppm.

### SEM Analysis

The morphologies of HPAM and AM/AA/NAE in aqueous solution at a concentration of 2000 mg/L were examined by SEM, as shown in Figure 4. The SEM images of HPAM are shown in Figure 4(a,c), and the AM/AA/NAE images are also shown in Figure 4(b,d). Figure 4(a) shows that the structure of HPAM was looser than that of AM/AA/NAE under the same conditions for 50 $\mu$m with an amplification factor of 5000 compared with Figure 4(b). A more legible structure of AM/AA/NAE is shown in Figure 4(c,d). Compared with the image of HPAM, a more close-knit structure, which clearly exhibited the three-dimensional networks, was observed. This phenomenon was mostly attributed to intermolecular or intramolecular associations and the crosslinking reactions among the macromolecule chains.

### Rheological Characteristics

**Shear Behavior.** The rheological properties of the 2000 mg/L polymer aqueous solution were measured by an RS 6000 rheometer with a shear rate ($\gamma$) from 3.7 to 1000 $s^{-1}$ at 25°C, and the results are presented in Figure 5(a). We observed that the viscosity of the two copolymers decreased sharply with increasing $\gamma$ from 3.7 to 200 $s^{-1}$. When we continued to raise $\gamma$ and the viscosity remained constant, they presented pseudoplastic behavior. However, we found that the curve of AM/AA/NAE was above that of HPAM, and the viscosity-constant value of the AM/AA/NAE was higher than that of HPAM during the high shear rate which might attribute to introduce the long hydrophobic chain N-allyloctadec-9-enamide (NAE) into the macromolecular and/or the hydrophobically associating interactions between the intra/intermolecular.

Meanwhile, we also investigated the shear resistance properties of AM/AA/NAE by changing $\gamma$ abruptly after we retained a constant $\gamma$ for 3 min, as shown in Figure 5(b). We observed that

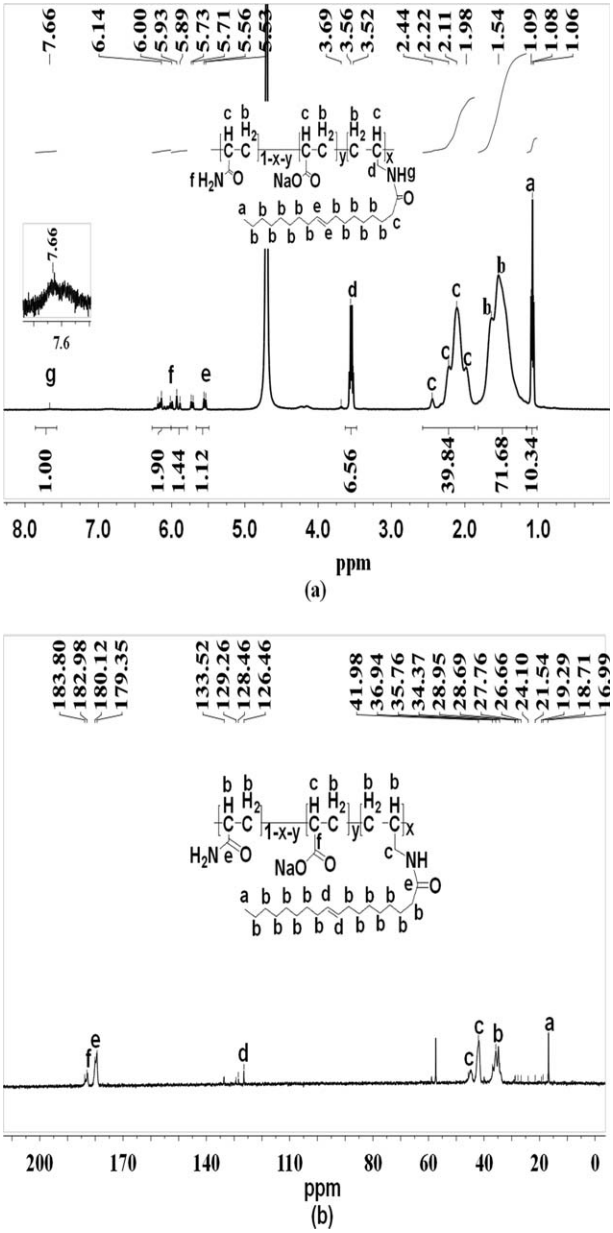


**Figure 3.** (a) $^1$H-NMR and (b) $^{13}$C-NMR spectra of AM/AA/NAE.

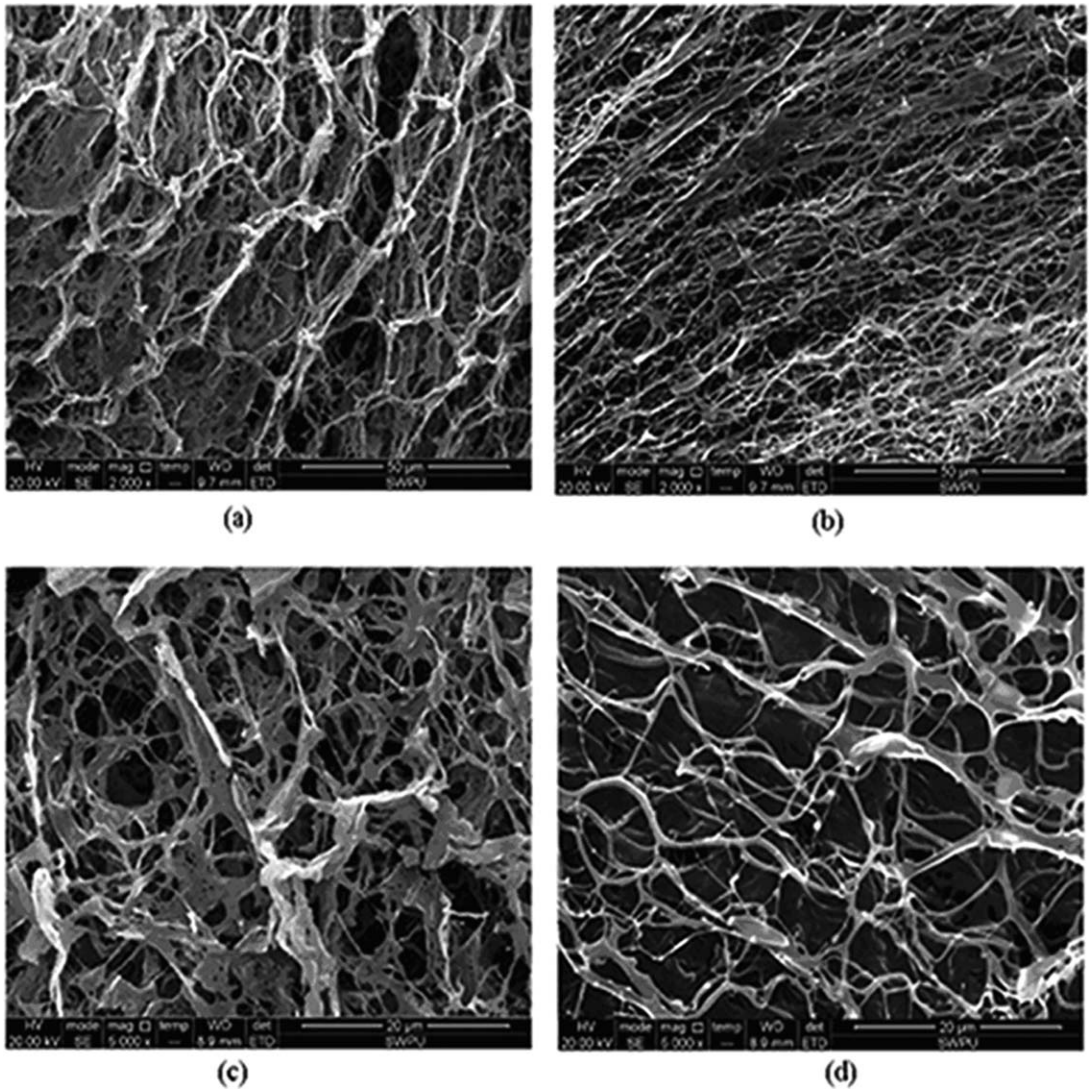


**Figure 4.** SEM images of HPAM and AM/AA/NAE: (a) HPAM, 50 $\mu$m; (b) AM/AA/NAE, 50 $\mu$m; (c) HPAM, 10 $\mu$m; and (d) AM/AA/NAE, 10 $\mu$m (concentration of copolymer = 0.2 wt %, temperature = 25°C, concentration of copolymer = 0.2 wt %, temperature = 25°C).

when $\gamma$ changed from 170 to 510 $s^{-1}$, the viscosity of HPAM was varied from 55 to 28 mPa s. When $\gamma$ was returned to 170 $s^{-1}$, the viscosity could only be restored to the original viscosity of 87% (48 mPa s at 170 $s^{-1}$). However, the viscosity of AM/AA/NAE ranged from 59 to 34 mPa s; this was higher than HPAM. Moreover, the viscosity almost returned to the original viscosity (59 mPa s at 170 $s^{-1}$) when one cycle was completed. This excellent performance could be explained by the fact that the intermolecular/intramolecular hydrogen bonding because the NAE structure could help regain the structure in AM/AA/NAE during shearing. This also suggested that AM/AA/NAE had the perfect property of retaining the viscosity and strong non-Newtonian behaviors; this was beneficial for injecting the polymer solution into assise in oil displacement.

**Stress Scanning.** Mathematically, the formula is known as the power law model [eq. (3)].[33] It demonstrates the relationship of the shear stress ($\tau$; Pa) with $\gamma$ ($s^{-1}$), which also was non-Newtonian.

$$\tau = k\gamma^n \tag{3}$$

where $k$ is the consistency coefficient (Pa $s^{-n}$) and $n$ is the flow behavior index. Taking logarithms, we could obtain eq. (4) as

$$\lg \tau = \lg k + n \lg \gamma \tag{4}$$

According to eq. (4), log $\tau$ and log $\gamma$ could show a straight-line relationship. The flow curves of 2000 mg/L aqueous solutions of AM/AA/NAE and HPAM, which accounted for the relationship between $\tau$ and $\gamma$, are shown in Figure 6. It is well known that most polymer solutions are generally classified as pseudoplastic fluids. The pseudoplastic material exhibited a smaller resistance to flow as $\gamma$ increased. In Figures 5(a) and 6, it is clear that the rheological behavior of the two polymers was a pseudoplastic fluid behavior that belonged to a non-Newtonian fluid; these are often used by chemical flooding agents.[26] After we did a

Applied Polymer SCIENCE

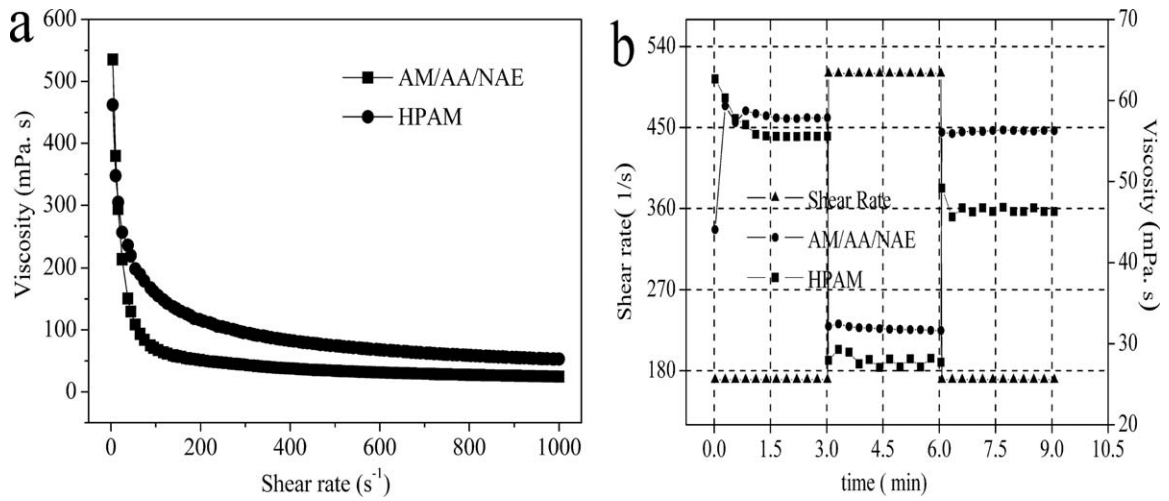


**Figure 5.** Effect of shearing on AM/AA/NAE in a water solution: apparent viscosity of (a) AM/AA/NAE and HPAM and (b) AM/AA/NAE in different $\gamma$s.

linear fitting of the graph processing, $n$ and $k$ were found to be 0.43 and 2.457 Pa $s^{0.43}$, respectively, for HPAM and 0.63 and 2.318 Pa $s^{0.63}$, respectively, for the AM/AA/NAE copolymer. Besides, oscillatory tests had conducted that the AM/AA/NAE solution was in the linear viscoelastic regime (detail information see supplementary material) and could be used in the filed of oil exploitation.

### Temperature Tolerance

What is more, the effect of the temperature on the AM/AA/NAE solution was studied with 2000 mg/L copolymer at a constant $\gamma$ of 170 $s^{-1}$ in Figure 7.

Figure 7 indicates that the results of viscosity for the AM/AA/NAE solution were greatly different those for HPAM. For the HPAM solution, the viscosity decreased in a straight manner with temperature up to about 80°C. However, for the AM/AA/NAE solution, it was interesting that the apparent viscosity gradually increased before 50°C. With further increases in temperature, the general trend showed a decrease in the apparent viscosity. The increase was likely due to the effect of the temperature on the change of interaction between macromolecules. When the temperature was lower, the intramolecular hydrophobic associations were dominant, and the intermolecular hydrophobic associations were slightly strengthened with increasing temperature. The viscosity retention rate reached 98% (79 mPa s) at 100°C. The excellent viscosity retention rate might be explained by the fact that a large number of associating groups aggregated together to form reversible, physical, supermolecular structures via strong van der Waal's interactions and/or polymer chains entangled with each other via hydrogen-bond interactions

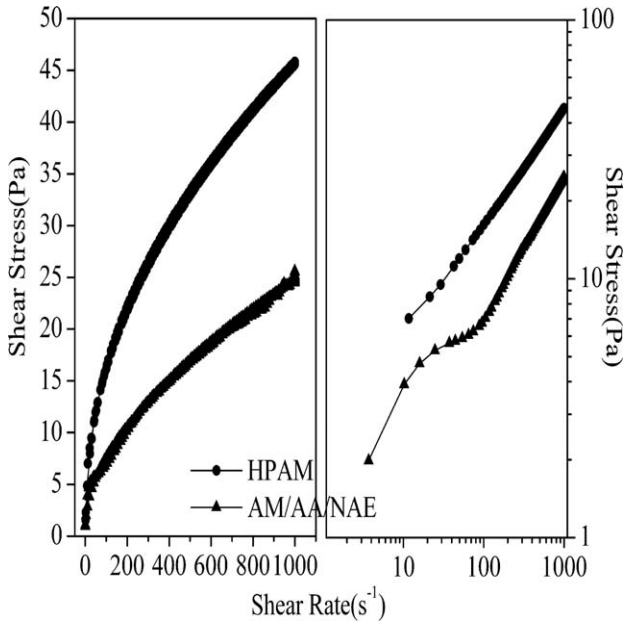


**Figure 6.** $\tau$ versus $\gamma$ for AM/AA/NAE at 25°C.

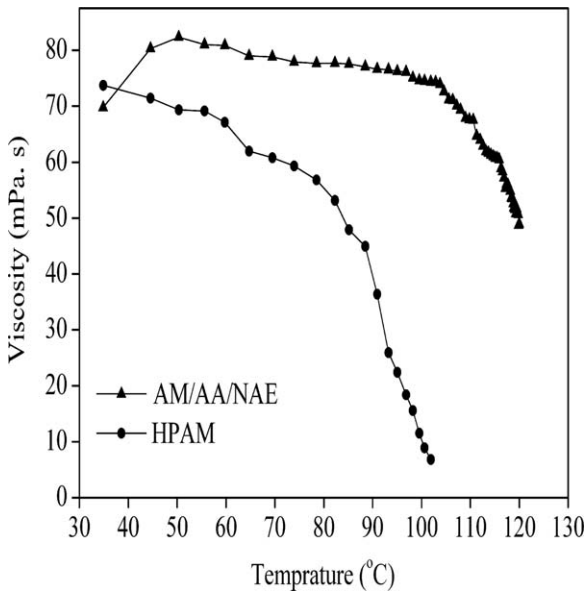


**Figure 7.** Results of the apparent viscosity of AM/AA/NAE and HPAM at different temperatures at 170 $s^{-1}$.

**Table II.** Resistance of AM/AA/NAE in Different Saline Waters

| Solvent | Polymer | $\eta_{water}$[d] (mPa s) | $\eta_{salt}$[e] (mPa s) | Viscosity retention rate (%) |
|---|---|---|---|---|
| Saline water[a] | HPAM | 259.3 | 94.4 | 36.4 |
| | AM/AA/NAE | 279.2 | 132.3 | 47.4 |
| Saline water[b] | HPAM | 259.3 | 72.9 | 28.1 |
| | AM/AA/NAE | 279.2 | 112.6 | 40.3 |
| Saline water[c] | HPAM | 259.3 | 29.0 | 11.2 |
| | AM/AA/NAE | 279.2 | 94.8 | 33.9 |

[a] Containing $[Na^+] = 5000$ mg/L, $[Mg^{2+}] = 100$ mg/L, and $[Ca^{2+}] = 100$ mg/L.
[b] Containing $[Na^+] = 5000$ mg/L, $[Mg^{2+}] = 300$ mg/L, and $[Ca^{2+}] = 300$ mg/L.
[c] Containing $[Na^+] = 5000$ mg/L, $[Mg^{2+}] = 500$ mg/L, and $[Ca^{2+}] = 500$ mg/L.
[d] $\eta_{water}$: the apparent viscosity of copolymer dissolved by pure water.
[e] $\eta_{salt}$: the apparent viscosity of copolymer dissolved by saline water.

in the aqueous solution. However, up to 115°C, the viscosity dropped markedly, and the retention rate was only 77%. The results reveal that AM/AA/NAE possessed the superior properties in temperature tolerance in the range from 90 to 100°C.

### Salt Resistance

The copolymer could be finally applied in the processes of oil recovery; nevertheless, the underground water accommodating an amount of inorganic ions, such as $Na^+$, $Ca^{2+}$, and $Mg^{2+}$, would be a vast influence on the properties of the copolymer.[26] $Ca^{2+}$ and $Mg^{2+}$ particularly have a great impact on the apparent viscosity of the copolymer. The aqueous solutions of HPAM and AM/AA/NAE were prepared with deionized water. Then, the salt solutions of the two polymers with different salinities, from 5200 to 6000 mg/L, were prepared with NaCl, $CaCl_2$, and $MgCl_2{\cdot}6H_2O$. The concentration of the polymers was 2000 mg/L. The viscosities of the mixture were measured by a Brookfield LVTDV-III viscometer at 7.34 $s^{-1}$ at 25°C, and then, the rate of viscosity retention of each polymer in the salt solution was calculated. The results are summarized in Table II.

According to the results in Table II, the viscosity of the two copolymers decreased generally with increasing salinity; this indicated that the intramolecular/intermolecular bindings (hydrogen and van der Waal's) decreased. In addition, we found that the viscosity retention rate of AM/AA/NAE was higher than that of HPAM when the salinity of the polymer solution increased. The different performance could be attributed to the fact that the intramolecular or/and intermolecular hydrophobic association effect strengthened the rigidity of macromolecule chains and prevented chains from curling under the high-salinity solution. Herein, we concluded that the salt resistance of AM/AA/NAE was better than that of HPAM.

### Pyrene Probe Fluorescence Spectrum of AM/AA/NAE

The ratio of the intensities between the first and the third vibronic peaks in the fluorescence spectrum of pyrene ($I_1/I_3$) was used[34] to estimate the micropolarity sensed by pyrene in its solubilization site. The fluorescence emission spectra of the pyrene probe sequences at 373, 379, 384, 390, and 410 nm near the five emission peaks are shown in Figure 8(a). Among them, $I_1/I_3$ decreased as the polarity of the solution decreased. This feature is often referred to as the pyrene *polarity scale*.[35,36] Therefore, $I_1/I_3$ was used to characterize the size of their environment polarity.

The fluorescence spectra of different concentrations of AM/AA/NAE are shown in Figure 8(b). Figure 8(c) depicts the dependence of the $I_1/I_3$ values of the pyrene steady-state fluorescence spectra on the copolymer concentration. The $I_1/I_3$ values remained almost constant when the concentration was lower than 0.65 g/L. When the concentration increased from 0.65 to 1.2 g/L, the $I_1/I_3$ values began to decrease significantly. The abrupt decrease in the $I_1/I_3$ values indicated that the pyrene molecules removed from the water bulk to the highly hydrophobic microdomains resulted from the formation of strongly hydrophobic associations.[37] A strong hydrophobic interaction occurring in the copolymer concentration was present when the CAC was above 0.65 g/L; this was also evident from the plots of the viscosity versus concentration shown in in Figure 8(d).

### Interactions between the Polymer and the Surfactant

The effects of the SDS, CTAB, and Tween-80 concentration on the interfacial tension and apparent viscosity of the AM/AA/NAE solutions are shown in Figure 9. The concentration of the polymer was maintained at 1000 mg/L, which was previously the CAC of the AM/AA/NAE solution. The interfacial tension curves of the SDS, CTAB, and Tween-80 solutions with concentration were also present when the critical micelle concentrations were 2000, 1200, and 5 mg/L, respectively; these were in agreement with published values.[38–40]

The interfacial tension and viscosity indicated that the AM/AA/NAE/SDS [Figure 9(a,b)] and AM/AA/NAE/CTAB systems [Figure 9(c,d)] gave dissatisfactory results in which the viscosity of these two kinds of systems sharply decreased with increasing concentration of the corresponding surfactants. In addition, the AM/AA/NAE/CTAB system gradually changed from transparent to turbid, and even the polymer was precipitated from the solution, as shown in Figure 9(e,f). This was attributed to the fact that the interaction between the cationic groups in CTAB and anionic —COONa in AM/AA/NAE was stronger with increasing concentration of CTAB; this resulted in the viscosity eventually being close to the water viscosity.

However, the AM/AA/NAE/Tween-80 system indicated that AM/AA/NAE interacted with Tween-80 as mixed micelles. The critical micelle concentration of the AM/AA/NAE/Tween-80 system was about 10 mg/L. This critical value was obviously lower than that of Tween-80. Moreover, the surface tension was minimum, and the apparent viscosity was maximum when the concentration of Tween-80 was the same; this showed evidence of the formation of high-surface activity aggregates. When the concentrations were previously the CAC, there was the comicellar network formation of the polymer and surfactant micelles because of the cooperative hydrophobic interaction.[41] The AM/AA/NAE/Tween-80 system indicated that viscosity enhancements were yielded by the addition of Tween-80. The reason might be the interaction between nonionic

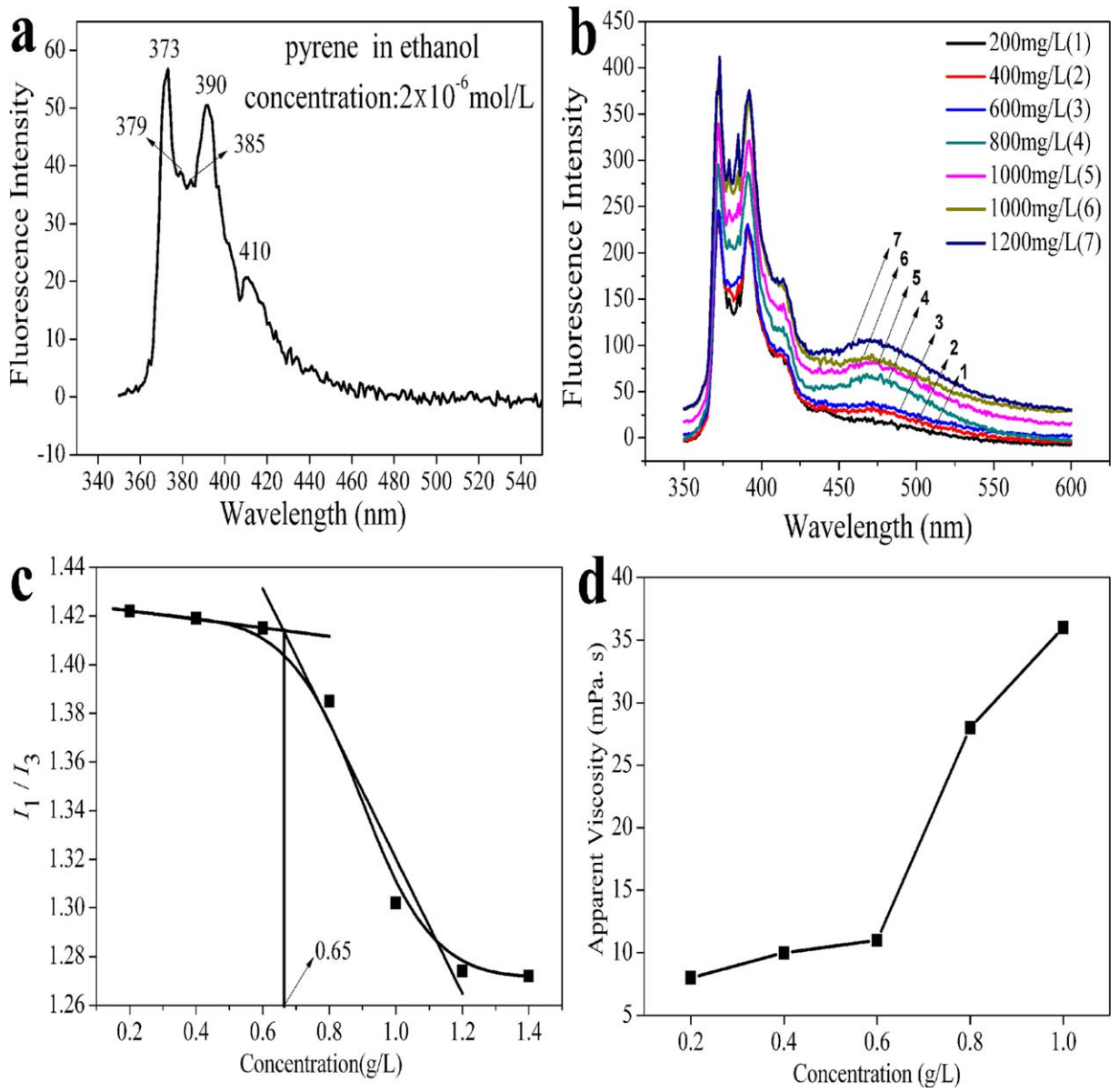


**Figure 8.** Hydrophobically associating behaviors of AM/AA/NAE in a water solution: (a) fluorescence spectrum of pyrene of $2 \times 10^{-6}$ mol/L in ethanol at 25°C, (b) fluorescence emission spectra of different concentrations of the copolymer solution at 25°C, (c) $I_1/I_3$ of the pyrene emission as a function of different concentrations for AM/AA/NAE, and (d) apparent viscosity of different concentrations for AM/AA/NAE at 7.34 $s^{-1}$ in deionized water. [Color figure can be viewed in the online issue, which is available at www.interscience.wiley.com.]

surfactants and AM/AA/NAE which was due to synergistic effect among the long hydrophobic chains of surfactants and polymer in this system. Besides, it was clearly found that the interfacial tension of AM/AA/NAE/Tween-80 system was markedly lower than the values of pure surfactant and HPAM/Tween-80 system. The possible reason might have been that the interaction of the hydrophobically associating effect was increased. As the hydrophobic structural units of NAE were introduced into the AM/AA/NAE macromolecular chain, the polymer could form comicelles with Tween-80. However, a lower surface tension value of the HPAM/Tween-80 system was not achieved; there may have been no hydrophobic units existing in the structure of HPAM.

**Adsorption Experiment**

Solutions at different concentrations were prepared with HPAM or a blend of AM/AA/NAE and the nonionic surfactant Tween-80. Γ of the surfactant to stratum was calculated on the basis of eq. (2). The results are displayed in Figure 10.

In general, Figure 10 shows that the absorbance of surfactant increased with increasing concentration, whereas the increasing rate gradually decreased on account of fewer adsorption sites and ultimately remained stable so we obtained the adsorption saturation. For only surfactant the adsorbance was large, which might be owned to the ability of Tween-80 permeating into rock was strong. However, in the HPAM/Tween-80 system, the electrostatic repulsion interaction between the —$COO^-$ group

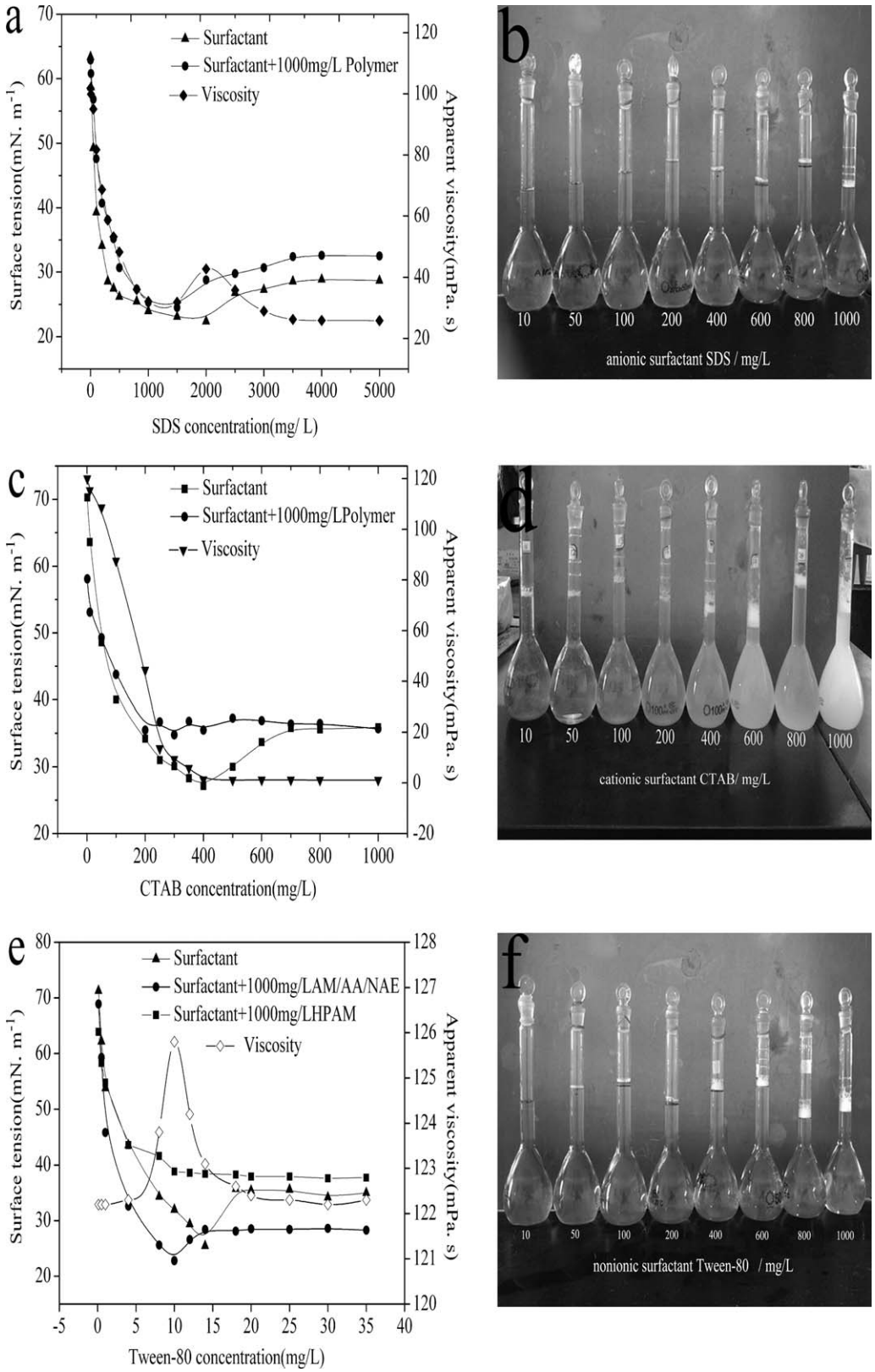


**Figure 9.** Plots of the surface tension and apparent viscosity against the surfactant concentration in the absence and presence of 2000 mg/L AM/AA/NAE: (a) SDS, (c) CTAB, and (e) Tween-80. Images of different concentrations of different surfactants in the presence of 2000 mg/L AM/AA/NAE: (b) SDS, (d) CTAB, and (f) Tween-80.

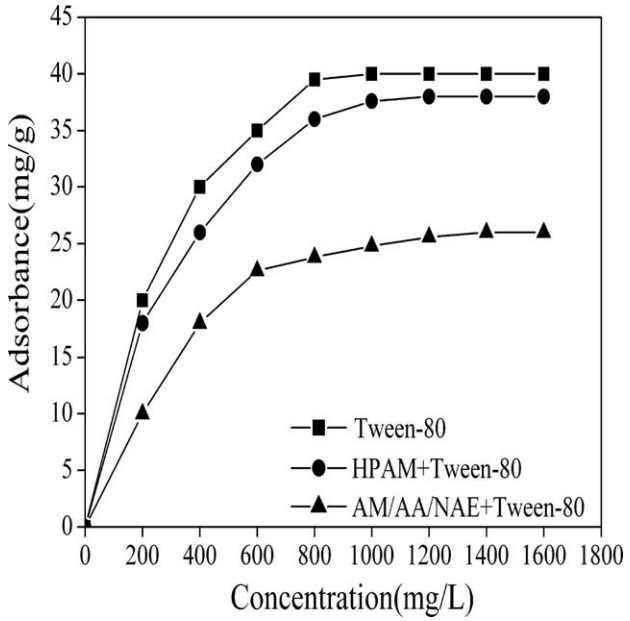


**Figure 10.** Γ curves.

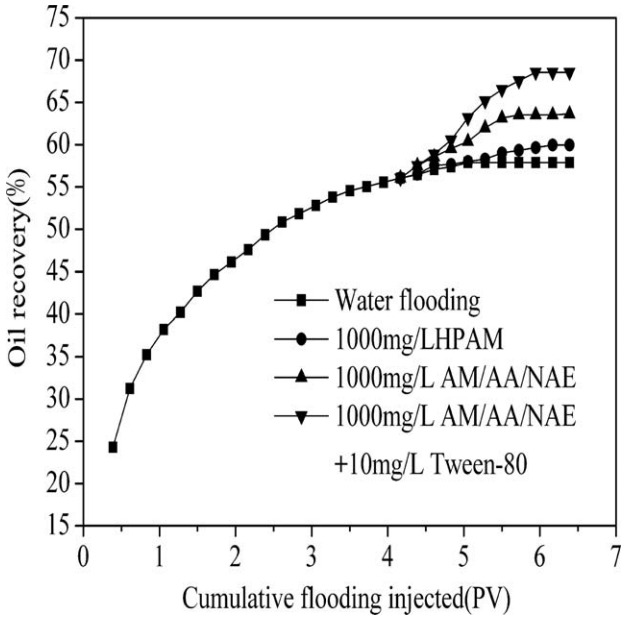


**Figure 11.** Results of the core flood tests of different systems in the laboratory experiment.

in the HPAM molecules and the negative charge carried on the surface of rock caused lower Γ than the pure surfactant solution. AM/AA/NAE significantly decreased the adsorption of the surfactant. This might have been due to the two following aspects: one was the repulsion force between the —$COO^-$ group in the AM/AA/NAE molecules and the negative charge of the rock surface, another was the hydrophobic associating interactions between AM/AA/NAE and Tween-80, which resulted in the enhancement of the interaction.

### Core Flood Test

The purpose described in this section was to investigate the properties of the polymer and polymer–surfactant system in enhanced oil recovery via the one-dimensional sand-packed model.[26] Concentrations of 1000 mg/L of HPAM, 1000 mg/L of AM/AA/NAE, and 1000 mg/L of AM/AA/NAE+10 mg/L Tween-80 solutions were used in the core flood tests. All of the results are shown in Figure 11. The value for enhanced oil recovery (EOR) was obtained with the following formula:

$$EOR = H_1 - H_2 \quad (5)$$

where $H_1$ is the oil recovery of polymer flooding and $H_2$ is the oil recovery of water flooding.

From the diagram compared with an oil recovery of about 56% in the brine system, we found that values of about 63.6% for recovery and 7.6% for EOR were revealed in 1000 mg/L AM/AA/NAE in the presence of 5000 mg/L NaCl brine at 65°C. However, the results of the application of HPAM under the same conditions were only about 60% for recovery and only 4% for EOR. A higher EOR result (12.5%) could be afforded with the use of the 1000 mg/L AM/AA/NAE + 10 mg/L Tween-80 system, and the oil recovery reached 68.5%; the results were obviously superior to those of HPAM.[42] The excellent performance may have greatly attributed to the characteristic comicellization/complex formation of the polymer and surfactant.

## CONCLUSIONS

A novel hydrophobically associating water-soluble copolymer, AM/AA/NAE, was synthesized via free-radical copolymerization. The optimum conditions were investigated and were as follows: [AM] = 16 wt %, [AA] = 4 wt %, [NAE] = 0.3 wt %, [OP-10] = 0.03 wt %, initial temperature = 40°C, pH = 7.5, [initiator] = 0.3 wt %, and reaction time = 8 h. The viscosity retention rate of AM/AA/NAE was up to 92% at a temperature of 100°C and was 43% at a $\gamma$ of 1000 $s^{-1}$. Also, the viscosity retention rate of the copolymer was 33.9% when the concentration of salt ions containing $Na^+$, $Ca^{2+}$, and $Mg^{2+}$ was 6000 mg/L. Furthermore, the AM/AA/NAE/Tween-80 system effectively reduced the interfacial tension and decreased the surfactant loss caused by stratum absorption. In the core flood test, the AM/AA/NAE/Tween-80 system showed that EOR was up to 12.5% in the presence of 5000 mg/L NaCl brine at 65°C. All of the results indicate that AM/AA/NAE had wider potential application for enhancing oil recovery in high-temperature and high-mineralization oil fields. Further investigation into the applications of the corresponding copolymers is ongoing.

## ACKNOWLEDGMENTS

The authors gratefully acknowledge the Natural Science Foundation of China (contract grant numbers U1262209 and 51274172) and the Sichuan Province Science and Technology Support Plan (contract grant number 2012FZ0130) for financial support and Nanjun Lai for core flood tests.

## REFERENCES

1. Jan Bock, D. B.; Siano, P. L.; Valint, S.; Pace, J. *Adv. Chem.* **1989**, *22*, 425.
2. Abu-Sharkh, B. F.; Yahaya, G. O.; Ali, S. A.; Kazi, I. W. *J. Appl. Polym. Sci.* **2001**, *82*, 467.

3. Shashkina, Y. A.; Zaroslov, Y. D.; Smirnov, V. A.; Philippova, O. E.; Khokhlov, A. R.; Pryakhina, T. A.; Churochkina, N. A. *Polymer* **2003**, *44*, 2289.
4. Yang, Q. B.; Song, C. L.; Chen, Q. *J. Polym. Sci. Part B: Polym. Phys.* **2008**, *46*, 2465.
5. Zhao, Y. Z.; Zhou, J. Z.; Xu, X. H.; Liu, W. B.; Zhang, J. Y.; Fan, M. H.; Wang, J. B. *Colloid Polym. Sci.* **2009**, *287*, 237.
6. Wang, Y. Y.; Dai, Y. H.; Zhang, L.; Luo, L.; Chu, Y.; Zhao, P. S.; Li, M. Z.; Wang, E. J.; Yu, J. Y. *Macromolecules* **2004**, *37*, 2930.
7. Castelletto, V.; Hamley, I. W.; Xue, W.; Sommer, C.; Pedersen, J. S.; Olmsted, P. D. *Macromolecules* **2004**, *37*, 1492.
8. Duan, M.; Hu, X. Q.; Ren, D. M. *J. Polym. Sci. Part B: Polym. Phys.* **2005**, *43*, 709.
9. Ye, L.; Li, Q.; Huang, R. H. *J. Appl. Polym. Sci.* **2006**, *101*, 2953.
10. Hill, A.; Candau, F.; Selb, J. *Macromolecules* **1993**, *26*, 4521.
11. Creutz, S.; Teyssié, P.; Jérôme, R. *Macromolecules* **1997**, *30*, 6.
12. Islam, M. F.; Jenkins, R. D.; Bassett, D. R.; Lau, W.; Ou-Yang, H. D. *Macromolecules.* **2000**, *33*, 2480.
13. Jiang, J.; Ram, M.; Chun, H. L.; Min, Y. L.; Ralph, H. C.; Dilip, G.; Miriam, H. R.; Jonathan, C. S.; Daniel, C. *Macromolecules* **2008**, *41*, 3646.
14. Evani, S.; Rose, G. D. *Polym. Mater. Sci. Eng.* **1987**, *57*, 477.
15. Zou, C. J.; Zhao, P. W.; Lei, Y.; Ye, H.; Yao, Y. L.; Chen, M. Q.; Wang, T. Y. *Chem. Eng. Technol.* **2011**, *34*, 1820.
16. Aubry, T.; Moan, M. *Macromolecules* **1998**, *31*, 9072.
17. Huaitian, B.; Kjøniksen, A. L.; Knudsen, K. D.; Nystrom, B. *Langmuir* **2005**, *21*, 10923.
18. Liu, J. X.; Guo, Y. J.; Hu, J.; Zhang, J.; Lv, X.; Zhang, X. M.; Xue, X. S.; Luo, P. Y. *Energy Fuels* **2012**, *26*, 2858.
19. Bai, G.; Wang, Y.; Yan, H.; Thomas, R. K.; Kwak, J. C. T. *J. Phys. Chem. B* **2002**, *106*, 2153.
20. Hayakawa, K.; Murata, H.; Satake, I. *Colloid Polym. Sci.* **1990**, *268*, 1044.
21. Bai, G.; Catita, J. A. M.; Nichifor, M.; Bastos, M. *J. Phys. Chem. B.* **2007**, *111*, 11453.
22. Kim, D. H.; Kim, J. W.; Oh-Kim, S. G.; Han, S., H.; Chung, D. J.; Suh, K. D. *Polymer* **2007**, *48*, 3817.
23. Pate, D. W.; Jarvinen, K.; Urtti, A.; Jarho, P.; Fich, M.; Mahadevan, V.; Jarvinen, T. *Life Sci.* **1996**, *58*, 1849.
24. Boger, D. L.; Sato, H.; Lerner, A. E.; Gao. X. J.; Gilula, N. B. *Bio. Med. Chem. Lett.* **1999**, *9*, 115.
25. Nedjhioui, M.; Moulai-Mostefa, N.; Morsli, A.; Bensmaili, A. *Desalination* **2005**, *185*, 543.
26. Ye, Z. B.; Gou, G. J.; Gou, S. H.; Jiang, W. C.; Liu, T. Y. *J. Appl. Polym. Sci.* **2013**, *128*, 2003.
27. Yang, F.; Li, G.; He, Y. G.; Ren, G. X. *Carbohydr. Polym.* **2009**, *78*, 95.
28. Bu, H.; Kjøniksen, A. L.; Knudsen, K. D.; Nyström, B. *Langmuir* **2005**, *21*, 10923.
29. Jiménez-Regalado, E.; Selb, J.; Candau. F. *Langmuir* **2000**, *16*, 8611.
30. Aubry, T.; Moan, M. *Macromolecules* **1998**, *31*, 9072.
31. Nedjhioui, M.; Moulai-Mostefa, N.; Morsli, A.; Bensmaili, A. *Desalination* **2005**, *185*, 541.
32. Yao, T.; Yao, F.; Li, J. *Oil Drill Prod. Technol.* **2008**, *30*, 82.
33. Zhang, L.; Zhang, D.; Jiang, B. *Chem. Eng. Technol.* **2006**, *29*, 395.
34. Gao, B. J.; Guo, H. P.; Wang, J.; Zhang, Y. *Macromolecules* **2008**, *41*, 2890.
35. Yu, X. Z.; Fei, P. W.; Miao, Z. L.; Er, J. W. *J. Phys. Chem. B.* **2005**, *109*, 22250.
36. Yang, Q. B.; Song, C. L.; Chen, Q.; Zhang, P. P.; Wang, P. X. *J. Polym. Sci. Part B: Polym. Phys.* **2008**, *46*, 2465.
37. Yekta, A.; Duhamel, J.; Brochard, P.; Adiwidjaja, I. H.; Winnik, M. A. *Macromolecules* **1993**, *26*, 1829.
38. Aniansson, E. A. G.; Wall, S. N.; Almgren, M.; Hoffmann, H.; Kielmann, I.; Ulbricht, W.; Zana, R.; Tondre, J. L. C. *J. Phys. Chem.* **1976**, *80*, 905.
39. Tuttle, T. R. *J. Phys. Chem.* **1971**, *86*, 3905.
40. Hu, F. Z.; Chen, G. R.; Du, Y. J. Interface of Materials; East China University of Science and Technology: Shanghai, **2007**; p 78.
41. Che, Y. J.; Tan, Y. B.; Ren, X. N.; Xin, H. P.; Meng, F. *J. Colloid Polym. Sci.* **2012**, *290*, 1237.
42. Wave, D. A. Z.; Picchioni, F.; Broekhuis, A. A. *Prog. Polym. Sci.* **2011**, *36*, 1558.